Crack identification with parametric optimization of entropy & wavelet transformation

Buddhi Wimarshana[a], Nan Wu[*] and Christine Wu[b]

Department of Mechanical Engineering, University of Manitoba, Winnipeg, Manitoba, R3T 5V6, Canada

Abstract. A cantilever beam with a breathing crack is studied to improve the breathing crack identification sensitivity by the parametric optimization of sample entropy and wavelet transformation. Crack breathing is a special bi-linear phenomenon experienced by fatigue cracks which are under dynamic loadings. Entropy is a measure, which can quantify the complexity or irregularity in system dynamics, and hence employed to quantify the bi-linearity/irregularity of the vibration response, which is induced by the breathing phenomenon of a fatigue crack. To improve the sensitivity of entropy measurement for crack identification, wavelet transformation is merged with entropy. The crack identification is studied under different sinusoidal excitation frequencies of the cantilever beam. It is found that, for the excitation frequencies close to the first modal frequency of the beam structure, the method is capable of detecting only 22% of the crack depth percentage ratio with respect to the thickness of the beam. Using parametric optimization of sample entropy and wavelet transformation, this crack identification sensitivity is improved up to 8%. The experimental studies are carried out, and experimental results successfully validate the numerical parametric optimization process.

1. Introduction

Identification of structural damages, which refers to detection and evaluation of these damages such as cracks, notches and delaminations, especially at their earliest stage is a vital process in engineering to avoid calamitous and irreparable damages. Bearing this in mind for the last few decades, structural health monitoring (SHM) with different damage identification techniques have been a largely concerned field of study for numerous researches from both industrial and academic communities. Global vibration-based structural damage detection methods are of a great interest due to their on-line real-time continuous damage detection capabilities, ability of monitoring literally any structural part of interest and their cost effectiveness during long runs (Kim and Stubbs 2003, Kim *et al.* 2007, Nagarajaiah and Erazo 2016, Providakis *et al.* 2015, Zhao *et al.* 2016).

---

*Corresponding author, Assistant Professor, E-mail: Nan.Wu@umanitoba.ca
[a]MSc. Student, E-mail: senakebw@myumanitoba.ca
[b]Professor, E-mail: Christine.Wu@umanitoba.ca

Vibration signals of a structure carries great amount of information about the healthiness of that particular structure. Most vibration-based structural damage detection methods strive to extract these damage related vibration information effectively and to interpret the damage which causing them. Yan *et al.* (2007) give a review on these vibration-based structural damage detection methodologies. They point out that modern vibration-based methods which are derived using signal processing techniques on measured online responses with intelligent damage identification agents such as artificial neural networks (ANNs) (Hakim and Razak 2013) and genetic algorithms (GAs) (Merunae and Heylen 2011) have more potential in evolving them as the damage detection schemes of the future over traditional vibration-based methods which are based on direct changes in the modal parameters of the structure, such as modal frequencies (Lee and Chung 2000). Wavelet analysis is also a popular signal processing method used in damage detection (Wang and Deng 1999, Yi *et al*. 2013). During a recent study, Wimarshana *et al.* (2016) also presented a high sensitivity vibration-based damage detection method derived from dynamic response processing using wavelet transformation (WT) with sample entropy (SampEn) as the damage quantification agent for detecting breathing cracks.

Fatigue cracks are evident as breathing cracks in many occasions of structural damages. During vibration of the structure with sufficient amount of deflection of the structure around the crack, the crack undergoes opening and closing repetitively which is generally termed as breathing phenomenon. Modeling this breathing phenomenon has been a topic for numerous researches (Abraham and Brandon 1995, Cheng *et al.* 1999, Wang *et al*. 2012) and a mathematical modeling technique combined with an iterative process has been developed by Wu (2015) and the method claims generating accurate reproduction of bi-linear dynamic properties of the breathing fatigue cracks computationally. The same modeling technique is used in the present study to generate temporal vibrational signals of a breathing crack cantilever beam. This breathing phenomenon of the crack imposes weak bi-linearity in the dynamic response of the structure introducing irregularities to the response.

Entropy is a measure, which can quantify the irregularity in system dynamics. Higher the complexity of a dynamic response of a given system, higher the entropy values are. Numerous entropy measures have been introduced since its introduction into dynamic systems by Kolmogorov (1958) and Sinai (1959). Sample entropy is a result of continuous studies on mitigating two major problems in experimental data: noise and lesser number of data available. Moreover, SampEn provides an improved evaluation of time series regularity (Richman and Moorman 2000). Therefore, SampEn can be employed as the main tool in proposed high-sensitivity crack identification process.

Entropy is employed as a tool to detect cracks by Yang *et al* (2013). The crack they considered is limited only to open cracks, and direct employment of entropy limited their approaches effective only for larger cracks. It is noted that the direct Entropy measurement on the structural dynamic response has low sensitivity to the occurrence of the breathing crack (Wimarshana *et al.* 2016). In the previous study done by Wimarshana *et al.* (2016), the concept of entropy is established for the first time as a high sensitivity breathing crack identification method. As an efficient technique to amplify the perturbations or irregularities in signals (Wang and Deng 1999), WT is introduced as a pre-data analyzer in improving the crack detection sensitivity. The current study aims to further improve the sensitivity of the proposed technique by Wimarshana *et al.* (2016) with lower vibration frequencies close to the first modal frequency of the structure by optimizing the parameters in SampEn and WT. The organization of this paper is as follows: in section 2 the overall crack identification methodology using entropy and WT is introduced and the theoretical

formulations of the mathematical tools used in this paper are given. Section 3 shows the details about the in-house experimental setup which is used to obtain the experimental results. Then, in section 4, the results pertaining to numerical studies conducted on parametric optimization of SampEn and WT is presented first and then the experimental results are given to validate the parametric optimization process. Finally, section 5 concludes the results and gives some suggestions on the future works.

2. Methodology of damage identification with entropy

In the current study, a vibrating cantilever beam with a breathing crack (near the fixed end) is studied. A schematic diagram of the beam structure is shown in Fig. 1.

The beam is considered as an ASTM A36 steel beam of a unit length (in meters). The cross section is $b \times h$, where b and h are the width and the thickness of the beam, respectively. The distance to the breathing fatigue crack from the fixed end is L_c, and it should be noted that, in this study, the crack is considered to be on the top surface of the cuboid shaped slender beam. The depth of the crack or crack severity (h_c) is varied in the analysis from zero (healthy beam) to half of the beam thickness ($h/2$). The crack depth percentage is the percentage ratio of the crack depth, h_c, to total thickness, h, of the beam. Young's modulus of the beam is E and density is denoted by ρ. The beam is excited sinusoidally at its free end. The angular frequency of the excitation is ω and the time elapsed is denoted using t. The overall crack identification process is described in the following section.

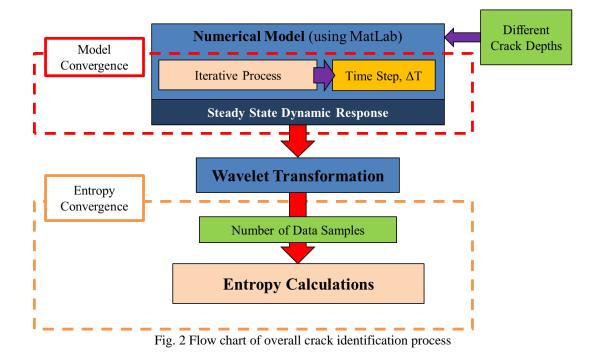### 2.1 The overall process of crack depth identification

Breathing phenomenon of the fatigue cracks introduces the repetitive crack opening/closing and the change of the structure stiffness during the vibration leading to weak bi-linearity in the dynamic response of the beam. This imposes irregularities/perturbations in the vibration signals, which can be quantified by the entropies of these signals. It is actually a measure of crack severity since these irregularities are directly related to the depth of the crack. It is noted entropy itself is not sufficient enough to correlate the severity of the crack because of the weak signatures of the perturbations generated by the breathing cracks. However, once these weak perturbations are magnified using WT, those correlations can be easily found using the entropy measures of respective wavelet transformed vibration signals. This proposed method is illustrated in Fig. 2 (Wimarshana *et al.* 2016).

Fig. 1 Cantilever beam with a breathing crack

As it is shown in Fig. 2, the first step of the derivation of the crack identification process is, building a mathematical model of the cantilever beam to obtain the vibration response of the tip of the beam considering the crack breathing with damping, and more details about the mathematical model can be found in section 2.2. Since the breathing process is a bi-linear problem, the vibration response of the mathematical model is obtained using an iterative method (Wu 2015). The accuracy of the dynamic response depends on the time step length used in the iterative process. Wu 2015 claims the convergence of dynamic responses as long as the iterative time step is smaller 0.001 seconds. Therefore, a time step of 0.0001 seconds is used in the current study. Then, by considering the damping effect during the vibration of the cantilever beam, the steady state response of the vibration signal is obtained and used for the entropy analysis. It should be noted that even though it is called 'steady state', it is not a pure steady state, rather a 'semi-steady state'. The breathing phenomenon introduces extra axial force when the crack goes from open-to-close position during vibrating. In addition to that, the stiffness (Eq. (7)) around the crack varies between the open and closed crack stages of the vibrating beam (more details about these two stages are described in section 2.2). Now due to these two reasons, perturbations appear in the vibration signal during the open-to-close and close-to-open stage transitions of the beam. Therefore it is never possible to have a pure steady state in the presence of a breathing crack. For the simplicity, this semi-steady state will be stated as 'steady state' throughout the paper.

It is noted that the direct Entropy measurement on the structural dynamic response is not sensitive to the occurrence of breathing crack (Wimarshana *et al.* 2016). The WT can help to magnify the weak bi-linearity in the vibration signal due to the breathing phenomenon of the crack so as to improve the Entropy measurement sensitivity for breathing crack identification (a description about WT is given in section 2.4). Therefore, the steady state vibration signal is first sent through WT. The transformed signal, WT coefficients, is then used in entropy calculations to

Fig. 2 Flow chart of overall crack identification process

quantify the irregularity of the vibration signal. The entropy measure used in the quantification process is SampEn and section 2.3 presents more details about SampEn. The convergence of the entropy calculations with the number of sampled vibration signal is obtained with 20,000 data samples.

The same crack detection process is carried out repeatedly for the crack depths ranging from zero (i.e., healthy beam) to half of the thickness of the beam (50% crack depth percentage) in 1% of crack depth percentage intervals. At each crack depth percentage, the percentage increment of the SampEn with respect to the healthy beam is calculated. Throughout the paper this value will be termed as 'percentage increment of SampEn'. The results corresponding to the correlations between the crack depth and the percentage increment of SampEn values for different excitation frequencies of ω are presented and discussed in depth in Wimarshana *et al.* (2016). In this study, those results are further improved by optimizing the parametric values of SampEn and WT, which are introduced in the following sections and discussed in depth in section 4.

2.2 Mathematical modeling of the cantilever beam with a breathing crack

As shown in Fig. 1, a cantilever beam of length L and uniform cross section of $b \times h$ is considered. The breathing crack is located at L_c from the fixed end and the depth of the crack is h_c. According to the Euler-Bernoulli beam theory, the governing beam equation is

$$EI\frac{\partial^4 w_{(x,t)}}{\partial x^4} + \rho A\frac{\partial^2 w_{(x,t)}}{\partial t^2} = F(x,t) \tag{1}$$

where I and A are the inertia moment of cross section and cross sectional area respectively. $w(x,t)$ is the vibration deflection of the beam at a distance of x from the fixed end at time t and the dynamic loading applied at the beam tip is $F(x,t)$.

First, when the slope on the left side of the crack is larger than the slope on the right side, the crack is in closed position, hence the beam can be treated as a healthy beam [31]. Then using variable separable method the mode shapes of the beam with the closed crack can be found for n^{th} mode of vibration

$$0 \le x \le L : W_{n,h}(x) = A_1\cos\beta_{n,h}x + A_2\cos\beta_{n,h}x + A_3\cos\beta_{n,h}x + A_4\cos\beta_{n,h}x \tag{2}$$

where A_1, A_2, A_3 and A_4 are unknown constants to be determined using boundary conditions and $\beta_{n,h}$ is given as

$$\beta_{n,h}^{\ 4} = \frac{\rho A}{EI}\omega_{n,h}^{\ 2} \tag{3}$$

and $\omega_{n,h}$ is the nth mode modal frequency of the 'healthy' beam (closed crack). Applying the boundary conditions of the cantilever beam in Eq. (2) give us four linear equations and we can solve them to find the nth natural frequency of the beam, $\omega_{n,h}$, and the corresponding modal shape, $W_{n,h}(x)$, for the closed crack position.

Secondly, when the slope of the left side of the crack is smaller than the right side, the crack is in open position and then the beam can be treated as an open crack beam or a damaged beam (Wu 2015). Now the beam is separated into two sections at the crack location to find the modal frequencies and the corresponding modal shapes. Let's assume that beam section to the left of the

crack as section 1 and the section to the right as section 2. Then, the vibration mode shapes of the two beam sections with open crack are

$$0 \leq x \leq L_c : W_{n,d1}(x) = A_5 \cos\beta_{n,d}x + A_6 \cos\beta_{n,d}x + A_7 \cos\beta_{n,d}x + A_8 \cos\beta_{n,d}x$$

$$L_c \leq x \leq L : W_{n,d2}(x) = A_9 \cos\beta_{n,d}x + A_{10} \cos\beta_{n,d}x + A_{11} \cos\beta_{n,d}x + A_{12} \cos\beta_{n,d}x \tag{4}$$

and $\beta_{n,d}$ is given as

$$\beta_{n,d}{}^4 = \frac{\rho A}{EI}\omega_{n,d}{}^2 \tag{5}$$

where $\omega_{n,d}$ is the nth mode modal frequency of the 'damaged' beam (open crack). The eight boundary conditions required to solve Eq. (4), are as follows

$$x = 0: \quad W_{d1}(x) = 0, \qquad \frac{dW_{d1}(x)}{dx} = 0;$$

$$x = L_c: \quad W_{d1}(x) = W_{d2}(x), \qquad \frac{dW_{d1}(x)}{dx} + \Theta L \frac{d^2 W_{d1}(x)}{dx^2} = \frac{dW_{d2}(x)}{dx},$$

$$\frac{d^2 W_{d1}(x)}{dx^2} = \frac{d^2 W_{d2}(x)}{dx^2}, \quad \frac{d^3 W_{d1}(x)}{dx^3} = \frac{d^3 W_{d2}(x)}{dx^3}; \tag{6}$$

$$x = L: \quad \frac{d^2 W_{d2}(x)}{dx^2} = 0, \qquad \frac{d^3 W_{d2}(x)}{dx^3} = 0$$

The parameter Θ represents the additional non-dimensional flexibility of the beam due to the opening crack (Wu 2015), which is defined as a function of the crack depth and calculated from fracture mechanics and Castigliano's theorem (Krawczuk and Ostachowicz 1995)

$$\Theta = 6\pi \frac{h}{L} \int_0^{h_c/h} x \left(\frac{0.923 + 0.199(1 - \sin(\frac{\pi}{2}x))^4}{\cos(\frac{\pi}{2}x)} \right)^2 \frac{\tan(\frac{\pi}{2}x)}{\frac{\pi}{2}x} dx \tag{7}$$

Substituting Eq. (4) into boundary conditions of the cantilever considering the crack opening given in Eq. (6), the nth natural frequency of the beam, $\omega_{n,d}$, and the corresponding modal shape, $W_{n,d}(x)$, can be solved.

Then, the full vibration response of the beam can be found using the mode superposition

$$w(x,t) = \sum_{n=1}^{\infty} W_n(x) q_n(t) \tag{8}$$

where n is the mode number and $q_n(t)$ is the generalized coordinate part. The process of obtaining full vibration response of the beam using the novel iterative method is described briefly

in the following paragraphs.

As it was mentioned before, during the vibration beam undergoes two structural states, open crack (damaged beam) and closed crack (healthy beam) stages with different stiffness at the crack position. Due to this bi-linear behavior of the beam, vibrational characteristics of the beam keep changing. Hence, it is not easy to derive accurate analytical vibration solution of the beam subjected to external excitations with variable stiffness of the structure (Wu 2015). Therefore, an iterative numerical approach is used to find the final vibration solution ($w(x,t)$) of the beam. More details on iterative process are given in (Wu 2015). The full vibration responses of the closed crack and the open crack stages of the beam at the ith time step (t_i), considering damping (ζ is damping ratio), at any position (x) on the beam with the judgment of the crack breathing states are given below.

If the slope on the left side of the crack is larger than the slope on the right side (i.e. the closed crack/ healthy stage), the deflection of the beam is given by

$$w(x,t_i) = \sum_{n=1}^{\infty} W_{n,h}(x)q_{n,h}(t_i) \tag{9}$$

$$q_{n,h}(t_i) = e^{-\varsigma\omega_{n,h}(t_i-\tau)}(A_{n,h}\cos\omega_{n,h}t_i + B_{n,h}\sin\omega_{n,h}t_i) +$$

$$+ \frac{1}{\rho A b'_{n,h}\omega_{n,h}^d} \int_{t_{i-1}}^{t_i} e^{-\varsigma\omega_{n,h}(t_i-\tau)}Q_{n,h}(\tau)\sin[\omega_{n,h}^d(t_i-\tau)]d\tau \tag{10}$$

where, damped natural frequency is given by, $\omega_{n,h}^d = \sqrt{1-\zeta^2}\,\omega_{n,h}$, $Q_{n,h}(\tau)$ is the generalized force function and given by, $Q_{n,h}(\tau) = \int_0^L F(x,t_i)W_{n,h}(x)dx$, $b'_{n,h} = \int_0^L W_{n,h}^2(x)dx$, and τ is a variable of time in Duhamel integration. In this iterative process, $A_{n,h}$ and $B_{n,h}$ are related to the vibration response from the previous iteration step

$$B_{n,h} = \frac{e^{\varsigma\omega_{n,h}t_{i-1}}\cos(\omega_{n,h}^d\,t_{i-1})\left(\dfrac{dq_n(t_{i-1})}{dt} + \varsigma\,\omega\,q_n(t_{i-1})\right) + q_n(t_{i-1})\,e^{\varsigma\omega_{n,h}t_{i-1}}\omega_{n,h}^d\,\sin(\omega_{n,h}^d t_{i-1})}{\omega_{n,h}^d}$$

$$A_{n,h} = \frac{q_n(t_{i-1})\,e^{\varsigma\omega_{n,h}t_{i-1}} - B_{n,h}\sin(\omega_{n,h}^d t_{i-1})}{\cos(\omega_{n,h}^d t_{i-1})} \tag{11}$$

$q_n(t_{i-1})$ terms in Eq. (11) is related with either healthy or damaged beam responses depending on the vibration state of the beam at the previous iterative time step.

On the other hand, if slope on the left side of the crack is smaller than the slope on the right side (i.e., the open crack/damaged stage), similar set of equations can be written as

$$w(x,t_i) = \sum_{n=1}^{\infty} W_{n,d}(x)q_{n,d}(t_i) \tag{12}$$

$$q_{n,d}(t_i) = e^{-\varsigma\omega_{n,d}(t_i-\tau)}(A_{n,d}\cos\omega_{n,d}t_i + B_{n,d}\sin\omega_{n,d}t_i) +$$

$$+ \frac{1}{\rho A b'_{n,d}\omega_{n,d}^d}\int_{t_{i-1}}^{t_i} e^{-\varsigma\omega_{n,d}(t_i-\tau)}Q_{n,d}(\tau)\sin[\omega_{n,d}^d(t_i-\tau)]d\tau \qquad (13)$$

where, $\omega_{n,d}^d = \sqrt{1-\zeta^2}\,\omega_{n,d}$, $Q_{n,d}(\tau) = \int_0^L F(x,t_i)W_{n,d}(x)dx$, $b'_{n,d} = \int_0^L W_{n,d}^2(x)dx$ and similar to the healthy beam stage stated before, $A_{n,d}$ and $B_{n,d}$ are related to the vibration response from previous iteration step

$$B_{n,d} = \frac{e^{\varsigma\omega_{n,d}t_{i-1}}\cos\left(\omega_{n,d}^d\,t_{i-1}\right)\left(\dfrac{dq_n(t_{i-1})}{dt}+\varsigma\,\omega\,q_n(t_{i-1})\right) + q_n(t_{i-1})\,e^{\varsigma\omega_{n,d}t_{i-1}}\omega_{n,d}^d\,\sin\left(\omega_{n,d}^d t_{i-1}\right)}{\omega_{n,d}^d}$$

$$A_{n,d} = \frac{q_n(t_{i-1})\,e^{\varsigma\omega_{n,d}t_{i-1}} - B_{n,d}\sin\left(\omega_{n,d}^d t_{i-1}\right)}{\cos\left(\omega_{n,d}^d t_{i-1}\right)} \qquad (14)$$

In Eqs. (9)-(14), the subscripts of n denotes the nth mode of the vibration, h and d denote the healthy and damaged vibration stages of the beam with closed and open crack, respectively. From the theoretical model described above, it is noticed that the beam structure with breathing crack keeps changing between the healthy and damaged stages repetitively with different natural frequencies and mode shapes during its vibration. The change of the structure during the vibration introduces additional irregularity of the vibration signal compared with the intact structure.

2.3 Sample entropy (SampEn)

Entropy can quantify the irregularity of time domain signals so as to detect and evaluate the breathing crack, which generates perturbations on the structural vibration signals. SampEn is capable in well handling of short, noisy data samples with trouble-free implementation (Richman and Moorman 2000). Let's take a time series X having N number of data points such as; $\{x(1), x(2), \dots, x(N)\}$, then its irregularity can be quantified as follows.

First, template vectors of length m ('m' is called embedding dimension) are defined, such as

$$X(1) = \{x(1), x(2),\dots, x(m)\}$$

$$X(2) = \{x(2), x(3),\dots, x(m+1)\} \qquad (15)$$

$$X(N-3+1) = \{x(N-m+1), x(N-m+2),\dots, x(N)\}$$

Then the Chebyshev distance between all template vectors are calculated, and lets denote it by $d[X_m(i), X_m(j)]$ and $i \neq j$. Then we define a parameter $B_i^m(r)$ as follows,

$$B_i^m(r) = \frac{\#\text{ of } j \text{ such that } \mathrm{d}[X_m(i), X_m(j)] \leq r}{N-m-1} \qquad (1 \leq j \leq N-m,\ j \neq i) \qquad (16)$$

where r is a pre-determined tolerance value taken as

$$r = k \times SD(X) \tag{17}$$

In Eq. (17), k is a constant $(k > 0)$ and SD stands for the standard deviation. Then we define

$$B^m(r) = (N - m)^{-1} \sum_{i=1}^{N-m} B_i^m(r) \tag{18}$$

Similarly, for template vectors of length $m + 1$

$$A_i^{m+1}(r) = \frac{\# \text{ of } j \text{ such that d}[X_{m+1}(i), X_{m+1}(j)] \le r}{N - m - 1} \qquad (1 \le j \le N - m, \, j \ne i) \tag{19}$$

and similar to Eq. (18)

$$A^{m+1}(r) = (N - m)^{-1} \sum_{i=1}^{N-m} A_i^{m+1}(r) \tag{20}$$

SampEn is then defined as

$$SampEn(m, r, N) = -\ln \left[\frac{A^{m+1}(r)}{B^m(r)} \right] \tag{21}$$

In this derivation, $B^m(r)$ is the probability that two sequences will match for m points, on the other hand, $A^{m+1}(r)$ is the probability of match for $m + 1$ points. Therefore, the quantity $[A^{m+1}(r)/B^m(r)]$ is the conditional probability that two sequences within a tolerance r for m points remain within r of each other at the next point (Richman and Moorman 2000). Higher the irregularity of the time series, then lower this value of conditional probability, hence we obtain a higher SampEn value.

2.4 Wavelet transformation (WT)

Wavelet transformation is a signal processing method, which can magnify the perturbations or irregularities in signals (Ren and Sun 2008) and be used to further enhance/support the entropy measurement to quantify the signal perturbations with higher sensitivity. The wavelet is a smooth and quickly vanishing oscillating function. WT maps a temporal signal, $f(t)$, into two-dimensional domain (the time-scale plane) and is denoted by $W_f(a, b)$ given by

$$W_f(a, b) = \frac{1}{\sqrt{a}} \int_{-\infty}^{+\infty} f(t) \; h^* \left(\frac{t - b}{a} \right) \; dt = \int_{-\infty}^{+\infty} f(t) \; h_{ab}^*(t) \; dt \tag{22}$$

where $h(t)$ is called the mother wavelet and the subscript * denotes the complex conjugate of the function. The basis functions of the transform, called daughter wavelets, are given by

$$h_{ab}(t) = \frac{1}{\sqrt{a}} h \left(\frac{t - b}{a} \right) dt \tag{23}$$

$h_{ab}(t)$ is a set of basis functions obtained from the mother wavelet $h(t)$ by compression or dilation using scaling parameter a and temporal translation using shift parameter b (Abbate *et*

al. 2002).

In the present study, we use the 'symlet2' as the mother wavelet function and WT is realized using the MatLab[®] software package.

2.5 Parametric study of SampEn and WT

In sections 2.3 and 2.4, it is noted that the entropy calculation and WT results depend on four parameters, m, k, WT scale and WT repetitions, which will affect the damage identification accuracy and sensitivity. The current study mainly focuses on the improvement of the damage identification sensitivity by changing the parametric values of SampEn and WT. In the results and discussion section, it can be found that the crack detection sensitivity for lower excitation frequencies (excitation frequencies close to the first modal frequency of the structure) is less compared to the higher excitation frequencies of the structure. Therefore, a parametric study of the proposed technique is carried out in results and discussions section to improve the crack detection sensitivity in lower excitation frequencies.

3. Experimental setup

To validate the results and conclusions obtained through numerical simulations, measurements on relevant aluminum alloy (grade 6061-T6) cantilever beams are conducted. The breathing fatigue cracks are constructed by bonding three aluminum alloy beams together; the same technique has been used by Prime *et al.* 1996 and Douka *et al.* 2005 to demonstrate breathing cracks experimentally. Fig. 3 illustrates the schematic arrangement of the bonded beam pieces for constructing the beam with a 25% crack depth percentage.

The crack is located 0.01 m from the fixed end of the cantilever beam, and the beam span is 1.00 m, which are same with the theoretical model. The healthy beam (0% crack depth percentage) is constructed by bonding two equivalent beams. This restricts the differences between healthy and cracked beams to the crack region (Prime *et al.* 1996). The final thickness of both healthy and 25% crack depth percentage beam are 0.00635 m (1/4 inches) and the width is 0.0254 m (1.00 inch).

Figs. 4 and 5 illustrates the experimental setup for obtaining the dynamic response from the 25% crack depth percentage beam. The beam is tightly clamped using four bolts to a steel
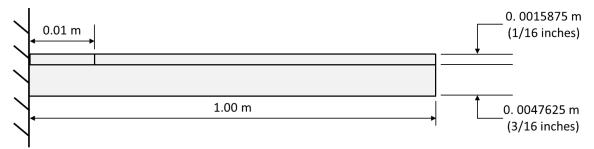

Fig. 3 Schematic diagram of the constructed test beam for 25% crack depth percentage
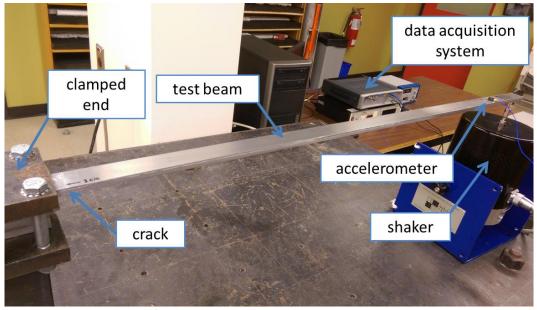
Fig. 4 The experimental setup for obtaining dynamic responses of damaged and healthy aluminum alloy cantilever beams
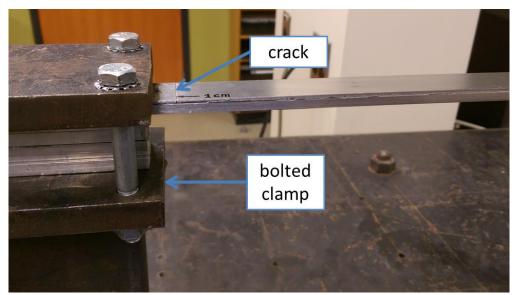

Fig. 5 The zoomed-in view of the crack area of the experimental beam setup

clamping post (see Fig. 5) which is solidly fixed to the concrete test bench. The free end of the beam is sinusoidally excited using a shaker (The Modal Shop - model 2100E11). PCB Piezotronics model 352A24 accelerometer weighing 0.8 g is located 0.10 m away from the free end of the beam. The sinusoidal signal generation and data acquisition are done using LMS SCADAS Mobile (type SCM05) data acquisition system and a personal computer.

4. Results and discussions

This section presents the results and corresponding discussions pertaining to the parametric study of the SampEn and WT on the breathing identification of the cantilever beam, which is described in section 2. The dimensions, material properties of the beam and vibration parameters are given in Table 1.

In our study, two excitation frequencies of the sinusoidal excitation at the free end of the beam, $F(t) = f\sin(\omega t)$, 45 rad/s (close to first modal frequency) and 300 rad/s (close to the second modal frequency), are chosen to show the excitation frequency effect on the crack identification sensitivity. The resultant percentage increment of the SampEn at each crack depth percentage with respect to the SampEn of the healthy beam is plotted and shown in Figs. 6-7. In here, crack depth percentage is the percentage ratio of the crack depth to the total thickness of the beam; i.e., 0%

Table 1 Dimensions and material properties of the cantilever beam

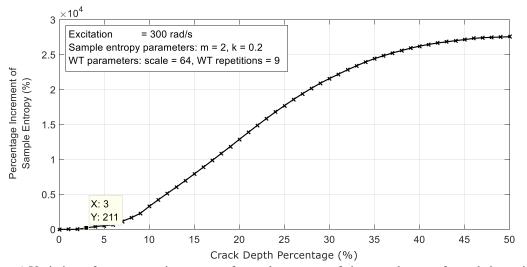| Parameter	Cantilever	Crack
L (m)	1.00	-
b (m)	0.05	-
h (m)	0.01	-
L_c (m)	-	0.01
h_c (m)	-	varies from 0.000 to 0.005 (in 0.0001 steps)
Young's modulus, E (GPa)	200	-
Density, ρ (kg/m^3)	8000	-
Equivalent damping ratio for the first three modes, ζ	0.01	-
Magnitude of the sinusoidal excitation, f (N)	10	-

Fig. 6 Variation of percentage increment of sample entropy of the wavelet transformed dynamic response for the excitation frequency of 300 rad/s (Wimarshana *et al.* 2016)
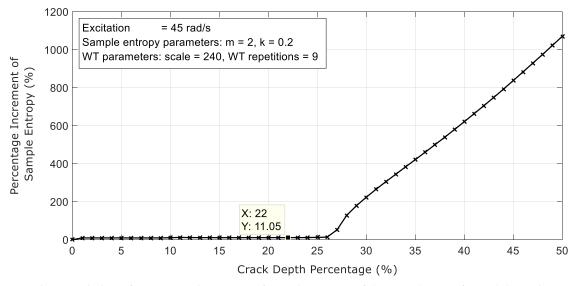
Fig. 7 Variation of percentage increment of sample entropy of the wavelet transformed dynamic response for the excitation frequency of 45 rad/s (Wimarshana *et al.* 2016)

crack depth percentage is the healthy beam and 50% crack depth percentage is a crack severity which penetrated half way through the total thickness of the beam.

Fig. 6 shows the percentage increment of the SampEn for the excitation frequency of 300 rad/s and the crack identification sensitivity (i.e., the smallest identifiable crack depth percentage ratio to the thickness of the beam) is just 3% of the crack depth percentage with a 211% of SampEn percentage increment. It is assumed that the cracks are only identifiable when the percentage increments of entropies due to the crack effect are more than 10% compared to the healthy beam. This is to keep some safe margin for the presumed degradation of the results of the proposed crack identification method, due to the inevitable environmental noises during the practical operation. On the other hand, Fig. 7 shows the percentage increment of the SampEn for the excitation frequency of 45 rad/s. This excitation is close to the first modal frequency of the beam. For this lower excitation frequency, the crack identification sensitivity is 22% of crack depth percentage with an 11% SampEn percentage increment. These results are also noticed in our previous study (Wimarshana *et al.* 2016) and suggest that the proposed crack identification technique has to be further improved for lower excitation frequencies in-order to improve the crack identification sensitivities at these excitations.

During the analysis it is found that variations of the percentage increment of SampEn (shown in Figs. 6-7) also depend on the parametric values used in SampEn and WT. SampEn employs two parametric values during the analysis process; viz. 'embedding dimension' (m) and 'k' value which varies the 'tolerance value' (r). In addition, two parameters in WT, 'WT scale' and 'WT repetitions'. Scale is the parameter used in WT to dilate or compress the wavelet (Eq. (23)). WT can be done any number of times one transformation after another, and 'WT repetitions' is the number of times the transformation done consecutively.

In this study, the four parameters are optimized step-by-step to improve the crack identification sensitivity of the proposed technique for the lower excitation frequency of 45 rad/s. The following

section presents the parametric optimization of SampEn.

4.1 Parametric optimization of SampEn

In the previous section, the parametric values used for SampEn to analyze 45 rad/s excitation are m=2 and k=0.2, and the parametric values for WT are scale=240 and WT repetitions=9. In this study, to improve the crack identification sensitivity at 45 rad/s, as the first step, the parametric values of SampEn are optimized. This is done using a traverse optimization algorithm; the flowchart of the algorithm is given in Fig. 8. The algorithm is implemented using MatLab® software package and the algorithm is explained in the following paragraphs.

First, the ranges for the parametric values of m and k are pre-defined. For m, the range is selected as from 2 to 10 with increments of 1. Therefore in Fig. 8, m_start (starting value of m) is 2 and m_end (ending/ limiting value of m) is 10. m_end is chosen as a fixed value since higher the value of m, more the computational time will be needed. For example, for a value of 2 for m, SampEn takes around 14 seconds to compute the calculation for 20,000 data samples (Wimarshana *et al.* 2016), using an Intel® Core i5 3.30 GHz personnel computer with 8 GB of random-access memory (RAM). Then, for a value of 4 for m, this time will be doubled approximately. Therefore, a value of 10 as the limiting value for m is appropriate considering the calculation efficiency. For k, k_start is 0.1 and k_end is 1 with an increment of 0.05. Once these ranges are set for the parametric values of SampEn, the algorithm requires a starting value for the crack depth percentage, h_p_start. During the analysis, this h_p_start is set as 3%, because that's the best crack identification sensitivity achieved for higher excitation frequencies in the previous study (Wimarshana *et al.* 2016).

Then, the algorithm calculates the percentage increment of SampEn at h_p_start crack depth percentage, initially using m_start and k_start values. If the percentage increment of SampEn is less than 10% at h_p_start crack depth percentage, the m and k values are incremented accordingly until this condition is satisfied. If this condition is satisfied for a certain value of m and k, at h_p_start crack depth percentage, then the same condition (i.e., whether percentage increment of SampEn is higher than 10%) is checked for the next 20 consecutive crack depth percentages in-order to achieve a smooth SampEn percentage increment for the next consecutive crack depths. If this is satisfied, then the corresponding m and k values are displayed and the variation of percentage increment of SampEn with 0% to 50% of crack depth percentages is plotted (a plot similar to Figs. 6-7). If the percentage increment of SampEn values are less than 10% for the whole range of m and k value for the crack depth percentage of h_p_start, then the crack depth percentage (h_p) is incremented by one (h_p=h_p_start+1). Then the same checks are done for the updated crack depth percentage as it is described earlier in this paragraph. The algorithm goes from one crack depth percentage to the next crack depth percentage while looping through the parametric values of m and k, looking for a better plot with better crack identification sensitivity. Due to this traversing optimization nature of the algorithm, the name 'traverse optimization algorithm' is coined by the authors. Fig. 8 gives the flowchart of the proposed Entropy parametric optimization algorithm. Fig. 9 shows the resultant graph from the algorithm.

The algorithm produced final optimized parametric values for m and k are 6 and 0.1 respectively. It can be seen from Fig. 9, with the new optimized parametric values of m and k, the crack identification sensitivity has been improved to 16% crack depth percentage with a 12% percentage increment of SampEn with respect to the healthy beam. (Before this parametric optimization for SampEn, this crack identification sensitivity was 22% with 11% in the percentage

increment of SampEn.) In addition, from Figs. 7 and 9, it should be noted that the percentage increment of SampEn values at 50% crack depth percentage has been improved from around 1000% to around 5000% with the parametric optimization.
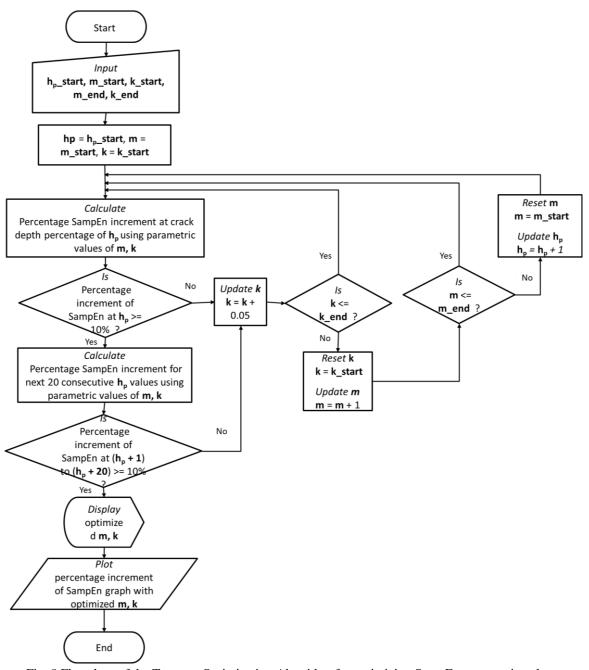

Fig. 8 Flowchart of the Traverse Optimization Algorithm for optimizing SampEn parametric values
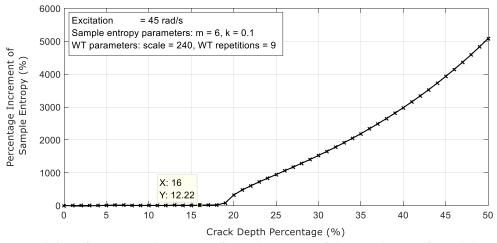
Fig. 9 Variation of percentage increment of sample entropy of the wavelet transformed dynamic response for the excitation frequency of 45 rad/s with optimized parametric values of SampEn

4.2 Parametric optimization of WT

WT has two parameters, WT scale and WT repetitions. During the analysis it is found that, these parameters have significant impact on the final crack identification sensitivity. The parametric optimization of WT is done and explained in the following paragraphs.

First, the percentage increment of SampEn variation with respect to WT scale and WT repetitions are observed using a three dimensional plot (3D plot). The 3D plot is graphed for the 16% crack depth percentage, which is the crack identification sensitivity achieved with parametric optimization of SampEn. This 3D plot is shown in Fig. 10.
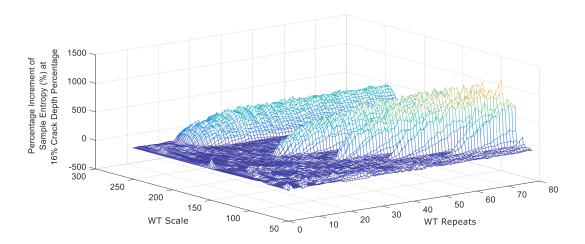

Fig. 10 Variation of percentage increment of sample entropy of the wavelet transformed dynamic response for the excitation frequency of 45 rad/s at 16% crack depth percentage
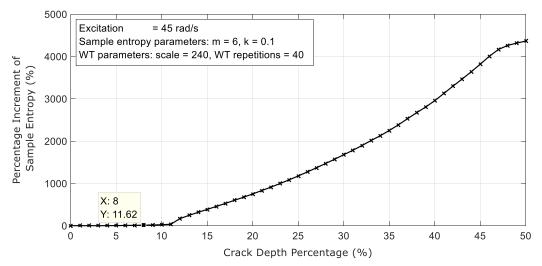
Fig. 11 Variation of percentage increment of sample entropy of the wavelet transformed dynamic response for the excitation frequency of 45 rad/s with optimized parametric values of SampEn and WT

It can be seen form Fig. 10 that percentage increment of SampEn (at 16% crack depth percentage) has some hills and valleys with the variation of WT scale and repetitions. Then, for the parametric optimization process, the WT scale and repetition ranges corresponding with the hills with high SampEn increment in the 3D plot are selected. As the next step, these ranges are given to another traverse optimization algorithm, which is similar to the algorithm explained in previous section. This algorithm optimizes the WT scale and repetition values such that the crack identification sensitivity is further improved. After the analysis, the algorithm produced final optimized parametric values for WT scale and WT repetitions as 240 and 40 respectively. The graph with improved crack identification sensitivity with optimized WT parametric values is shown in Fig. 11.

From Fig. 11 it can be seen that the crack identification sensitivity is improved to 8% crack depth percentage with an 11% percentage increment of SampEn with respect to the healthy beam. The crack identification sensitivity has been improved from 22% (for the non-optimized parametric values of both SampEn and WT) to 8% of crack depth percentage as a result of the final parametric optimization of both SampEn and WT.

Then, the numerical results for percentage increment of SampEn values at 25% crack depth percentage values obtained from Fig. 7 (i.e., result from non-optimized parametric values) and Fig. 10 (the final result from optimized parametric values) are compared with the experimental results for the 25% crack beam. This is done to verify the parametric optimization process experimentally, and the results are given in the next section.

4.3 Experimental verification of parametric optimization

In this section, the numerical results for percentage increment of SampEn using optimized and non-optimized parametric values for both SampEn and WT are compared with experimental results. The experimental results are obtained using the experimental setup described in section 3.

Table 2 Comparison of numerical and experimental results for percentage increment of SampEn on the beam of 25% crack depth percentage with optimized and non-optimized parametric values

	Percentage increment of SampEn at 25% crack depth percentage compared with the healthy beam (%)	
	Using non-optimized parametric values of SampEn and WT (m=2, k=0.2, WT scale=240, WT repetition=9)	Using optimized parametric values of SampEn and WT (m=6, k=0.1, WT scale=240, WT repetition=40)
Numerical method	12	1175
Experimental method	9	59

The two experimental aluminum alloy cantilever beams, i.e., healthy beam and 25% crack depth percentage beam are excited with a frequency of 5.92 Hz which is close to the first modal frequencies of the two beams. Measurements include raw acceleration-time data for the two beams.

From the acceleration-time data collected for the two beams, 20,000 data points are selected. Then these data are analyzed for the percentage increment of SampEn with the two different settings of the parametric values. The first setting is the non-optimized parametric values with m=2, k=0.2, WT scale=240 and WT repetitions=9. And the second setting is the optimized parametric values with m=6, k=0.1, WT scale=240 and WT repetitions=40. The entropy increment results with different parameters from both simulation and experiments are compared and shown in Table 2.

Table 2 reveals that both numerical and experimental results (12% and 9% Entropy increment) are in good agreement with each other for the percentage increment of SampEn at 25% crack depth percentage with non-optimized parametric values of SampEn and WT. On the other hand, with the optimized parameters, significant improvement of the detection sensitivity is noticed for the 25% crack from both simulation and experimental studies. The SampEn increments of the vibration response due to the crack are enhanced to be 1175% and 59% from the simulation and experiment, respectively. It is noted that the experimental result is lower than the numerical result by a considerable value. This is due to the inevitable presence of environmental noise in the dynamic signal in the experimental testing.

The important thing to note here is, even though there is a considerable difference in numerical and experimental results for the optimized parametric values, there is a notable rise in the percentage increment of SampEn values with optimized parametric values from the experimental testing. This increment will definitely lead to higher crack identification sensitivity and be useful in crack identification process when the proposed method is employed in real world crack detection scenarios.

5. Conclusions

The high sensitivity breathing crack identification (detection and evaluation) of a beam structure is proposed and realized using entropy measures with parametric optimization. The crack identification sensitivity of the proposed methodology for lower excitation is further studied and

improved by optimizing the parametric values of SampEn and WT. The simulation and experimental study results conclude the following points.

(1) From simulation results, it is noted that using the parametric optimization, 8% crack depth percentage can be identified, which is much more sensitive compared with the case with non-optimized parametric values (22%).

(2) Experimental testing for the 25% crack case, results show an improvement in the crack identification sensitivity with the parametric optimization by the higher SampEn increment value (59%) compared to the non-optimized parametric case (9%). The experimental study in particularly validates the numerically optimized entropy and WT parameters.

The noise effect can be removed from the experimental dynamic signals by introducing an efficient filtering process, which will improve the experimental results significantly. This requires further study of the breathing phenomenon and better understanding of the perturbation signal frequencies induced by the crack breathing so that the filter can effectively remove the noise without erasing the breathing perturbations. This effective filter development is considered as a future work for the current research.

Acknowledgments

References

Abbate, A., DeCusatis, C.M. and Das, P.K. (2002), *Wavelets and Subbands: Fundamentals and Applications*, Birkhauser, Boston, Massachusetts, USA.

Abraham, O.N.L. and Brandon, J.A. (1995), "The modeling of the opening and closure of a crack", *J. Vib. Acoust.*, **117**(3A), 370-377.

Cheng, S.M., Swamidas, A., Wu, X.J. and Wallace, W. (1999), "Vibrational response of a beam with a breathing crack", *J. Sound Vib.*, **225**(1)**,** 201-208.

Douka, E. and Hadjileontiadis, L.J. (2005), "Time-frequency analysis of the free vibration response of a beam with a breathing crack", *NDT & E Int.*, **38**(1), 3-10.

Hakim, S.J. and Abdul Razak, H. (2013), "Structural damage detection of steel bridge girder using artificial neural networks and finite element models", *Steel Compos. Struct.*, **14**(4), 367-377.

Kim, J.T., Park, J.H., Yoon, H.S. and Yi, J.H. (2007), "Vibration-based damage detection in beams using genetic algorithm", *Smart Struct. Syst.*, **3**(3), 263-280.

Kim, J.T. and Stubbs, N. (2003), "crack detection in beam-type structures using frequency data", *J. Sound Vib.*, **259**(1), 145-160.

Kolmogorov, A.N. (1958), "New metric invariant of transitive dynamical systems and endomorphisms of lebesgue spaces", *Doklady of Russian Academy of Sciences*, **119**(5), 861-864.

Krawczuk, M. and Ostachowicz, W.M. (1995), "Modelling and vibration analysis of a cantilever composite beam with a transverse open crack", *J. Sound Vib.*, **183**(1), 69-89.

Lee, Y. and Chung, M. (2000), "A study on crack detection using eigenfrequency test data", *Comput. Struct.*, **77**(3), 327-342.

Meruane, V. and Heylen, W. (2011), "An hybrid real genetic algorithm to detect structural damage using modal properties", *Mech. Syst. Signal Pr.*, **25**(5), 1559-1573.

Nagarajaiah, S. and Erazo, K. (2016), "Structural monitoring and identification of civil infrastructure in the United States", *Struct. Monit. Maint.*, **3**(1), 51-69.

Prime, M.B. and Shevitz, B.W. (1996), "Linear and nonlinear methods for detecting cracks in beams", *Proceedings of 14th International modal analysis conference*, Michigan, February.

Providakis, C., Tsistrakis, S., Voutetaki, M., Tsompanakis, Y., Stavroulaki, M., Agadakos, J., Kampianakis, E. and Pentes, G. (2015), "A new damage identification approach based on impedance-type measurements and 2D error statistics", *Struct. Monit. Maint.*, **2**(4), 319-338.

Ren, W. and Sun, Z. (2008), "Structural damage identification by using wavelet entropy", *Eng. Struct.*, **30**(10), 2840-2849.

Richman, J.S. and Moorman, J.R. (2000), "Physiological time-series analysis using approximate entropy and sample entropy", *Am. J. Physiol.. Heart and circulatory physiology*, **278**(6), 2039-2049.

Sinai, Y.G. (1959), "On the notion of entropy of a dynamical system", *Doklady of Russian Academy of Sciences*, **124**, 768-771.

Wang, Q. and Deng, X. (1999), "Damage detection with spatial wavelets", *Int. J. Solid. Struct.*, **36**(23), 3443-3468.

Wang, W.J., Lu, Z.R. and Liu, J.K. (2012), "Time-frequency analysis of a coupled bridge-vehicle system with breathing cracks", *Interact. Multiscale Mech.*, **5**(3), 169-185.

Wimarshana, B., Wu, N. and Wu, C. (2016), "Application of entropy in identification of breathing cracks in a beam structure - simulation and experimental studies", *Struct. Hlth. Monit.*, (under review).

Wu, N. (2015), "Study of forced vibration response of a beam with a breathing crack using iteration method", *J. Mech. Sci. Technol.*, **29**(7), 2827-2835.

Yan, Y.J., Cheng, L., Wu, Z.Y. and Yam, L.H. (2007), "Development in vibration-based structural damage detection technique", *Mech. Syst. Sign. Proc.*, **21**(5), 2198-2211.

Yang, Z., Chen, X., Jiang, Y. and He, Z. (2013), "Generalised local entropy analysis for crack detection in beam-like structures", *Nondestructive Test. Evaluat.*, **29**(2), 133-153.

Yi, T.-H., Li, H.-N. and Gu, M. (2013), "Wavelet based multi-step filtering method for bridge health monitoring using GPS and accelerometer", *Smart Struct. Syst.*, **11**(4), 331-348.

Zhao, S., Wu, N. and Wang, Q. (2016), "Crack identification through scan-tuning of vibration characteristics using piezoelectric materials", *Smart Mater. Struct.*, **26**(2), 025005.

Zhao, S., Wu, N. and Wang, Q. (2016), "Damage detection of beams by a vibration characteristics tuning technique through an optimal design of piezoelectric", *Int. J. Struct. Stab. Dyn.*, **16**(10), 1550070.

JK